First steps to rationalize host-guest interaction between α-, β-and γ-cyclodextrin and divalent first row transition and post-transition metals (subgroup VIIB, VIIIB and IIB)

Héloïse Dossmann, Lucas Fontaine, Teddy Weisgerber, Véronique Bonnet, Eric Monflier, Anne Ponchel, Cedric Przybylski

First steps to rationalize host-guest interaction between α-, β- and γ-cyclodextrin and divalent first row transition and post-transition metals (subgroup VIIB, VIIIB and IIB)

Héloïse Dossmann[1], Lucas Fontaine[2], Teddy Weisgerber[2], Véronique Bonnet[2], Eric Monflier[3], Anne Ponchel[3] and Cédric Przybylski[1]*

1 Sorbonne Université, CNRS, Institut Parisien de Chimie Moléculaire, IPCM, F-75005 Paris, France

2 Université de Picardie Jules Verne, Laboratoire de Glycochimie, des Antimicrobiens et des Agroressources, LG2A, CNRS UMR 7378, 80039 Amiens, France.

3 Univ. Artois, CNRS, Centrale Lille, Univ. Lille, UMR 8181 -UCCS- Unité de Catalyse et Chimie du Solide, F-62300 Lens, France.

ABSTRACT: Cyclodextrins (CD) are cyclic oligosaccharides mainly composed of 6, 7 and 8 glucose units, so called α-, β- and γ-CD, respectively. They own a very particular molecular structure exhibiting hydrophilic features thanks to primary and secondary rims, and delimiting a hydrophobic internal cavity. This latter can encapsulate organic compounds, but the former can form supramolecular complexes by hydrogen bonding or electrostatic interactions. CDs have been used in catalytic processes to increase mass transfer in aqueous-organic two-phase systems or to prepare catalysts. In this last case, interaction between CDs and metal salts was considered as a key point to obtain highly active catalysts. Up to now, no work was reported on the investigation of factors affecting the binding of metal to CD. In the study herein, we present the favorable combination of electrospray coupled to mass spectrometry ESI-MS(/MS) and DFT molecular modeling (B3LYP/Def2-SV(P)) to delineate some determinants governing the coordination of first row divalent transition metals (Mn^{2+}, Co^{2+}, Ni^{2+}, Cu^{2+}, Fe^{2+}) and one post-transition metal (Zn^{2+}) with α-, β- and γ-CD. A large set of features concerning the metal itself (ionic radii, electron configuration and spin state) as well as the formed complexes (the most stable conformer, relative abundance in MS, CE_{50} value in MS/MS, binding energy, effective coordination number, average bond lengths, binding site localization, bond dissociation energies (BDEs) as well as natural bond orbital (NBO) distribution) were screened. Taking into account all of these properties, various selectivity rankings have been delineated, portraying differential association-dissociation behaviors. Nonetheless, unique 3-D topologies for each CD-metal complexes were emphasized. The combination of these approaches brings a stone for building a compendium of molecular features to serve as a suitable descriptor or predictor for a better first round rationalization of catalytic activities.

INTRODUCTION

Very often, biomolecules-based ligands use nitrogen or oxygen atoms as lone pair rich center in their various molecular interactions. In such a context, considerable efforts were done to use polyols, and more particularly carbohydrates, during transition metals based reaction such as catalysis or control of the chemical reactivity.[1,2] Nowadays, it is well known thanks to many earlier findings that the electrostatic interactions between the metal and ligating oxygen atoms are the dominant force governing the carbohydrate-metal non covalent complex formation.[3–6] Nevertheless, it is lesser understood if 3-D conformation of carbohydrates can provide a more and less particular template to afford specific or at least selective molecular recognition. In such context, growing interest was devoted during the two last decades towards an attractive carbohydrates subclass issued from biomass and commercially available named cyclodextrins (CDs).[7,8] Native CDs are cyclic carbohydrates where the well-known α-, β- and γ-CD are composed of 6, 7 and 8 α–(1→4)-linked D-glucopyranose units, respectively, leading to a characteristic doughnut-shaped structure (Figure 1). Such particular structure enables dual features: hydrophilic functions due to hydroxyl groups located on C-6 (primary rim) and C-2/C-3 (secondary rim) oriented towards the external environment. Such properties confer encapsulating abilities to CDs for a wide range of organic compounds[9,10] and enable the formation of adducts with inorganic metal salts,[11] which can find applications as capping agents or templates in the synthesis of various nanoparticles, materials and metallo-enzyme active site mimetics.[12–19] Numerous studies dealing with host-guest interaction involving CD and alkali metal have been

achieved successfully thanks to both experimental and theoretical approaches. The former involved mass spectrometry using Matrix-Assisted Laser Desorption Ionization (MALDI-MS)[20–22] or gentler ionization as Electrospray (ESI-MS),[23–25] and the latter mainly used Hartree–Fock (HF) and density functional theory (DFT) based methods.[26,27] On the other hand, some investigations also revealed that cations with valence higher or equal to 2 were particularly attractive, for example to enhance drug solubilization in aqueous

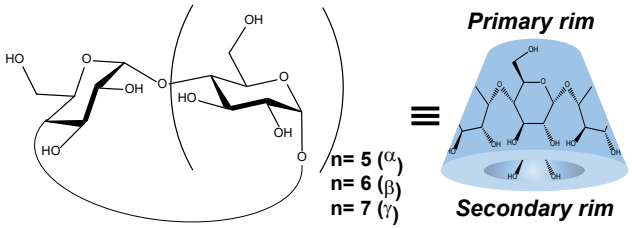

Figure 1. Structure of α-, β- and γ-cyclodextrins.

solution such as the addition of Mg^{2+} for doxycycline or quinolone,[29,30] or also to serve as a naked-eyes metal sensor tools for a large set of divalent and trivalent cations.[31] In this context, transition metals are of special interest as commonly associated with cyclodextrins as supramolecular hosts to act as organometallic catalysts.[32] One can for instance cite the combination of β-CD with Fe^{2+}, Co^{2+}, Ni^{2+}, Cu^{2+} and Zn^{2+} as improved catalysts in asymmetric aldol condensation reaction.[33] It was also demonstrated that the use of Cu^{2+} allows to form a coordinating complex with the β-CD secondary hydroxyl groups, leading to a highly regioselective method for preparing CD C-6 monosulphonyl derivative.[34] The theoretical study of complexation between CD and divalent metal cations was probed using DFT and could give rise to interesting features. Rogalski and coworkers demonstrated that complexation led to two groups of conformers depending on the metal used,[26] the first one (with Al^{3+}, Cu^{+} or Na^{+}) preserving the initial orientation of glucopyranose residues and the second one (with Mg^{2+} and Zn^{2+}), modifying their orientation consecutively to the ligand binding, showing the so-called induced-fit binding effect and insuring complex stability.[26,35] Recently, Dudev and co-workers have applied DFT implemented with a polarizable continuum model method to study the interaction between α-, β- and γ-CD with Na^{+}, Rb^{+}, Mg^{2+}, Sr^{2+}, Al^{3+} and In^{3+}.[27] They also experimented a DFT/continuum dielectric method combination to study the factors affecting complexation between α-CD with divalent alkaline earth metal (Be^{2+}, Mg^{2+}, Ca^{2+}, Sr^{2+} and Ba^{2+}) and post-transition metals (Zn^{2+}, Cd^{2+} and Hg^{2+}).[36] Both tailoring and characterization of homometallic CD-metal complexes are still in its infancy and a challenge for experimental chemists. In addition, native CDs form relatively low-stability complexes with metal centers in neutral aqueous solutions.[15] Such low stability has motivated the extensive functionalization of CDs with a large variety of ligands. That can be used to form CDs based metal complexes, providing efficient platform for molecular recognition and catalysis.[18-21]

Regarding more particularly complexes involving native CD and divalent transition metals, they were only studied in strongly basic conditions (pH >11).[11] To date, only one case in neutral aqueous solutions was reported with native β-CD and $CuCl_2$.[37] In such study, a stable molecular complex for CD/Cu(II) of stoichiometry 1:1 was observed by X-ray crystallographic analysis thanks to the coordination of copper by two chloride ions and two water molecules. More recently, Velasco *et al.* have characterized the physicochemical properties of native α-, β-, and γ-CD–CuX_2- assemblies (where X = Br^-, Cl^-, and NO_3^- anions) in dichloromethane, demonstrating also a 1:1 stoichiometry.[38] Some studies have unambiguously demonstrated that catalytic reactions can be affected either by the metal within β-CD-metal complexes or by the nature of native CD. For example, in the same conditions, β-CD with Fe(II), Co(II), Ni(II) and Zn(II) yield 48, 31, 83 and 37%, respectively, during aldol condensation.[33] On the other hand, Co(II) associated to α-, β-, and γ-CD yield 48, 73 and 64% during direct amination of alcohols.[12] Besides these few works, the state of art devoted to the understanding of the complexes involving both α-, β- and γ-CD and a wide set of transition metals commonly used under neutral or acidic aqueous conditions used in catalysis appeared surprising to us, quite poorly documented and it also emphasized the lack of systematic study made on these systems. In the study herein, we report efforts to fill this gap, by investigation of supramolecular assemblies of some divalent first row transition and post-transition metals (Table 1) with native α-, β- and γ-CD using a combination of ESI-MS, ESI-MS/MS and DFT. Our goal was to ascertain if some features such as metal properties as well as its most stable location, number of coordination points, O-metal bond lengths or also orientation of hydrogen bonds network could be suitable molecular descriptors. Such pieces of information will constitute a primer to enlighten parameters affecting recognition process. Then a set of selected parameters could serve as a possible first round rationalization of catalytic activities observed with some native CD/transition metal complexes.

MATERIALS AND METHODS

Chemical and reagents

α- and β-cyclodextrins were kindly provided by Roquette Frères (Lestrem, France). γ-cyclodextrin was kindly supplied by Wacker Chemie S.A.S. (Lyon, France). Cobalt(II) chloride hexahydrate ($CoCl_2$,· $6H_2O$) (98%), nickel(II) chloride hexahydrate ($NiCl_2$,· $6H_2O$) (99.9%), manganese(II) chloride tetrahydrate ($MnCl_2$·, $4H_2O$) (99.99%), zinc(II) chloride ($ZnCl_2$) (99.999%), copper(II) chloride (≥99.995%), iron(II) chloride (98%) were purchased from Sigma–Aldrich (Saint-Quentin Fallavier, France). Methanol (MeOH) used for sample preparation was HPLC grade and was purchased from VWR (West Chester, PA, USA).

Table 1. Recapitulative of some physico-chemical properties of studied metals.

Metal	Oxidation State (Z)	Geometry	CN[b]	Electronic configuration	Spin state	CIR[c] (pm)	Z/CIR	HIR[d] (pm)	Z/HIR
Mn	2	Octahedron	6 (83%), 4 (13%)	$[Ar]3d^5 4s^2$	High Low	0.83 0.67	2.41	4.38	0.46
Fe	2	Octahedron	6 (74%), 4 (18%)	$[Ar]3d^6 4s^2$	High Low	0.61 0.78	3.13-3.17	4.28	0.47
Co	2	Octahedron/cube	**6 (59%)**, 4 (34%)	$[Ar]3d^7 4s^2$	High Low	0.75 0.65	2.68 3.08	4.23	0.47
Ni	2	Octahedron	**6 (48%)**, **4 (48%)**	$[Ar]3d^8 4s^2$	-	0.69	2.90	4.04	0.50
Cu	2	Octahedron, JT[a]	5 (41%), 4 (34%)	$[Ar]3d^9 4s^2$ or $[Ar]3d^{10} 4s^1$	-	0.65	3.08	4.19	0.48
Zn	2	Octahedron	4 (59%), 6(23%)	$[Ar]3d^{10} 4s^2$	-	0.74	2.70	4.30	0.47

[a] JT: Jahn-Teller; [b] preferred metal coordination number (CN) with respective frequencies from the Cambridge Structural Database. The most common is indicated in bold and the percentages in parentheses, [c] Crystal ionic radius; [d] Hydrated ionic radius.[39]

Water was of ultrapure quality, obtained from a MilliQ apparatus (Millipore, Milford, USA).

ESI-MS(/MS) analysis

The electrospray-mass spectrometry (ESI-MS) experiments were performed using a LTQ-Orbitrap XL instrument from Thermo Scientific (San Jose, CA, USA) operated in positive ionization mode with a spray voltage at +3.85 kV and a sheath and an auxiliary gas flow at 45 and 15 a.u., respectively. Stock solutions of α, β and γ-CD and metal chloride were prepared at 1 mmol.L^{-1} and 200 mmol.L^{-1} respectively, in methanol/water (1:1 v/v). Then, each solution was diluted in methanol/water (1:1 v/v) to give final analytical solutions of cyclodextrin and metal chloride at 10 µM and 100 µM, respectively. Once prepared, the fresh solutions were continuously infused at 5 µl.min^{-1} using a 250-µL syringe. We assume that metal oxidation was negligible due to very short time scale analysis. The applied voltages were +40 and +100 V for the ion transfer capillary and the tube lens, respectively. The ion transfer capillary was held at 275 °C. The resolution level was set to 30,000 (m/z = 400) for all studies, while the m/z range was set to 300-2000 m/z in the profile mode and in the normal mass ranges during full scan experiments. The spectra were analyzed using XCalibur 2.0.7 acquisition software (Thermo Scientific, San Jose, CA, USA) without smoothing and background subtraction. High-energy collision dissociation (HCD) experiments were conducted with an activation time of 100 ms according to a previous study[40] and occurred in an octopole collision cell aligned to the C-trap. Detection was made in the Orbitrap in centroid mode. This dedicated cell was supplied with a rf voltage (2.6 MHz, 500 Vp-p), where the DC offset could be varied by 250 V and crossed with N_2 gas at a pressure of 5.10^{-3} mbar. The endcap voltage was controlled using normalized collision energy (NCE) technology, where the collision energy was modified for each experiment and was expressed in % of NCE. The peak-to-peak voltage was scaled as Vp-p =NCE/30 × (a(m/z) + b), where a and b are the instrument parameters set to 0.002 and 0.4, respectively. The standard range was 0% to 100% corresponding to 0-500 V. During the survival yield experiments, the NCE varied from 0 to 50%. The precursor selection window was set to m/z = 2.5 during the MS/MS experiments. The automatic gain control (AGC) allowed accumulation up to 10^6 ions for FTMS scans, 3.10^5 ions for FTMSn scans and 3.10^4 ions for ITMSn scans. The maximum injection time was set to 500 ms for both FTMS and FTMSn scans and 100 ms for ITMSn scans. For all scan modes, 1 µscan was acquired.

Molecular modeling

Electronic structure calculations were performed using the Gaussian 09 software package.[41] Due to the large amount of structures to be tested, a preselection of the most stable ones was first made using Hartree-Fock calculations with the 6-31G basis set. For each CD-complex (α, β or γ), 3 positions of the metal in the cavity were probed (lower/upper rim and in the middle of the truncated cone). Moreover, a supplemental degree of freedom occurs, since the possible orientations of the hydrogen bonds from primary to secondary rim of CD can be both clockwise (cw) or counterclockwise (cc). This leads to CD which can adopt six conformations (cwcw, cccc, cwcc, cccw and o_cccc and o_cwcw).[24,26,42] Further, for each metal, two spin states were also tested (singlet and triplet for Fe^{2+}, Ni^{2+} and Zn^{2+}, doublet and quadruplet for Co^{2+}, Mn^{2+} and Zn^{2+}). For all these combinations, geometry optimization and frequency calculation were done, the electronic energies obtained were compared and finally the 3 or 4 most stable complex for each metal + CD association were selected. Their structure and energy were then affined using the B3LYP hybrid functional coupled to the Ahlrichs 's Def2-SVP(P) basis set.[43]

RESULTS AND DISCUSSION

ESI-MS to portray the solution content

UV-Visible spectroscopy was used successfully as naked-eye detection for modified CD-metal complexes in solution

by Suresh *et al*.[31] Nevertheless, such approach to probe native CD-transition/post-transition metals was not conclusive (See Text S1 and Figure S1) and prompted us to steer on an alternative way such as MS. Several factors can influence the type and the intensity of metal complexes during MS, such as nebulization conditions (voltage, pressure and nature of drying gas) but especially, the solvent and the molecule/metal ratio. All these factors require to adequately select solution/instrumental parameters settings. In the absence of added salts, it is well known that full mass spectra of CD exhibit mono and doubly charged ions corresponding to adducts with protons, ammonium and some residual alkali metals (Na^+ and K^+).[24] We previously demonstrated that β-CD/$Co(NO_3)_2$ with 0.1 as CD/metal molar ratio provided the best results in term of intensity and signal to noise ratio regarding our optimized ESI-MS parameters.[44] Herein, the same molar ratio was used. In spite of such tuning, important differences in the MS spectra of the complexes of a given CD, with the six studied metals were obtained. As example, ESI-MS spectra of α-, β- and γ-CD with $MnCl_2$ or $ZnCl_2$ are presented in Figure 2. The other full scan MS spectra are given in supplementary information (Figure S2 to S4). All MS spectra reveal the presence of doubly charged ions assigned to $[CD+Metal]^{2+}$ and other numerous ions arising from the association of CD/metal/chloride in various stoichiometries and revealing that such complexes are enough stable to be detected by ESI. Moreover, we have detected the formation of $(CD)_x/(metal)_y$ complexes with x=1 or 2 and y = 1, 2 or 3, but we further investigated only the CD/metal 1/1 complexes, since they are by far, the most abundant within MS spectra. It was also noted that the background signal, composed of free clusters of metallic salts was more or less intense depending on the CD-metal formulation. As experimental conditions were strictly identical, we postulated that such differences could come from two main factors: (i) various solubility/dissolution behaviors of metal•Cl_2 in methanol/water solution and/or (ii) intrinsic affinity difference of the metals toward cyclodextrins, leading to more or less free metals. Ion ascribed to monoprotonated $[CD+H]^+$ could also sometimes be detected and may be due to proton release from action of metals on methanol as protic solvent. This observation was supported by the substitution of methanol by acetonitrile which was shown to avoid protonated adduct formation but considerably reduced solubility (data not shown). Interestingly, varying concentration of metal salts with or without CD unambiguously demonstrated that CD is required to form some high content metal chloride based supramolecular complex, such as for example in the case of electrosprayed β-CD + $ZnCl_2$ solution (Figure 2E). Because of the absence of available complexation constants for these systems, we assumed that equal ionization efficiencies take place and that relative response of the overall spectrum reflects a suitable portray of the solution content once the solvent molecules are evaporated. Therefore, extracting abundance of the ion $[CD+M]^{2+}$ from full MS spectra of α-, β- and γ-CD with the six metal chloride solutions allows to establish the following apparent affinity ranking for α-CD: $Ni^{2+} > Cu^{2+} > Fe^{2+} > Mn^{2+} > Co^{2+} > Zn^{2+}$ and for β-CD and γ-CD: $Ni^{2+} > Cu^{2+} > Fe^{2+} > Zn^{2+} > Co^{2+} > Mn^{2+}$. Interestingly, as observed for some cyclofructans which are analogs in size with α-CD and β-CD, no correlation was observed between the relative stabilities of the complexes and the crystal ionic radius (CIR) of Ni^{2+}, Fe^{2+}, Co^{2+}, Zn^{2+} and Cu^{2+} (Table 1).[45]

DFT based Molecular modeling

To get further insight into the structural parameters governing the stability of CD-transition metal complexes in gas phase, DFT calculations were performed (see materials and methods section).[24,26,42] When the metals is initially set in the middle of the truncated cone and in the secondary rim, it moves to the narrow rim suggesting that this is the most stable location.

Similarly, several spin multiplicities of metal were systematically screened including singlet (S), doublet (D), triplet (T) and quadruplet (Q). Nonetheless, even if various spin multiplicities can naturally occurred for a given metal, only one electronic configuration seems to lead to the most stable complex i.e. S for Fe^{2+} and Zn^{2+}, D for Ni^{2+} and Cu^{2+} and Q for Mn^{2+} and Co^{2+}. Abundance order obtained in ESI-MS spectra was confirmed by molecular modeling using B3LYP/Def2-SV(P) based DFT calculation where binding energy (E_{ass}) of the most stable complexes varied from -377.0 to -326.6 kcal.mol^{-1}, -397.9 to -328.3 kcal/mol and -412.9 to -336.5 kcal.mol^{-1} for α-, β- and γ-CD, respectively (Table 2). It must also be kept in mind, that difference between the three most stable conformers, taking into account E_{ass} for a given CD+metal complex, varied in a 4.5-32.5 kcal.mol^{-1} range (Table S1). For all complexes, DFT data indicate that the cations were stabilized by three, four or five electron-donating oxygens i.e. the number of coordination points (NCP). As example, three O-metal bonds are observed in the $[\alpha\text{-CD} + Cu]^{2+}$ complex and have estimated bond lengths (BL) of 1.933, 1.933 and 2.150 Å corresponding to an average BL of 2.005 Å. These three bonds involve 6-hydroxyl groups of consecutive glucose units (Table 2 and Figures 3). Similar behavior occurred for $[\alpha\text{-CD} + Mn]^{2+}$ and $[\alpha\text{-CD} + Ni]^{2}$, involving four 6-hydroxyl groups. Conversely, for $[\alpha\text{-CD} + Co]^{2+}$, the four O-Co bonds involve only three consecutive glucoses as "n", "n+1" and "n+2" position, but where the glucose in "n" position shares simultaneously both it 6-hydroxyl group and it hemiacetal oxygen. In addition, most of the time, binding of divalent transition metal leads to a deformation of the α-, β- and γ-CD cavity (Figures 3-5). This is presumably due to the coordination of the cation at one side of the primary rim CD rather than in the center. An exception occurred with $[\gamma\text{-CD} + Mn]^{2+}$, where the cation is almost located at the center of the primary rim with a slightly deeper position, but still inducing an important carbohydrate backbone deformation. Such results are in good agreement with previous studies on other divalent cations, where better binding are obtained with metal localized at the primary rim level following the central axis without any tilt, as exemplified for Mg^{2+} and Sr^{2+}.[27,36] On the other hand, there is a dramatic lack of experimental data for CD/$Metal^{2+}$ 1/1 complexes, because of the difficulty to isolate such systems. At our

knowledge and as indicated in the introduction, there is only one reported X-ray structure, corresponding to an hydrated β-CD/ $CuCl_2(H_2O)_2$ complex.[37] The comparison of this structure with our calculated gas-phase β-CD/Cu^{2+} can thus only be roughly qualitative, because of the composition difference and the bonding mode of the two complexes. In our gas-phase complex, the Cu^{2+} ion indeed binds to oxygens of the CD, whereas the $CuCl_2(H_2O)_2$ moiety does not established covalent bond with the CD rim. In this case, two main differences appears which are due to the different nature of the two involved guests. First, a larger upper rim diameter can be observed for β-CD/$CuCl_2(H_2O)_2$ (12.895 Å) compared to that of β-CD/Cu^{2+} (10.257 Å) (Figure S5) . This feature is coherent with the inclusion of a large guest ($CuCl_2(H_2O)_2$) in the first complex and also by the repulsive effect that the chloride atoms play on the closest CH_2-OH. Furthermore, the β-CD/Cu^{2+} complex appears to have a less regular structure, due to the covalent bonding of Cu^{2+} to the CD, which tends to deform the shape of the rim.

As coordination of one metal cation supports cycle deformations leading to tight binding, the rest of CD backbone shall appear more contracted and consequently more exposed to external dissociation agents. Such behavior was further investigated by probing gas phase stability using ESI-MS/MS.

Probing gas phase stability

The fact that ions detected by MS could not necessary portray the solution content is still under debate. However, some strong evidences were recently given, especially by the recently introduced ion-mobility technique. The survival yield methodology, which was initially developed to correlate conditions in the mass spectrometer to the internal ion energies,[46] can serve as a versatile tool to achieve a relative comparison of strength between a ligand and a receptor. A survival yield (SY) experiment consist in selecting a given ion as 100% precursor, and then to gradually increase the energy provided to the system (MS/MS). This yields a progressive diminishment of precursor intensity for the benefit of corresponding fragments. A SY value equal to 50% reflects the amount of energy required to be transferred to the precursor ion such that the reaction rate results in 50% decomposition. As the rate constant is dependent on the structure of the precursor ion, such value usually known as CE_{50}, will be presumably dependent on the molecular structure of the precursor ion.[40,45,47–50] Such values have been previously used to differentiate the stabilities of transition metal/cyclofructans complexes and discriminate analytes such as linear and cyclic maltodextrins, by means of size for a given geometry or also isomers.[40,45,49,50] More recently, it was successfully applied to study selectivity of alkali metals towards native and variously methylated β-CD.[24] Moreover, it must be kept in mind that the SY approach can be used on a similar manner with a given analyte in presence of one or multiple ligands i.e. results were not influenced by several complexes which simultaneously occurred. HCD mode provides a "triple quadrupole like" fragmentation mechanism which offers a fine tuning to monitor carbohydrate decomposition such as oligomaltosides and native α-, β- and γ-CD.[14] From a practical point of view, the SY was calculated following equation 1:

$$SY\ (\%) = (I_0)/(\Sigma I_X + I_P) \times 100 \quad \text{equation (1)}$$

With: I_0, is the intensity of the peak of the precursor ion after excitation with 0% NCE, I_P, the intensity of the precursor ion after excitation at a given normalized collision energy and ΣI_x is the sum of intensity of the various fragments at the same NCE. Experimental points were next fitted to plot a sigmoid curve to extract CE_{50}. In addition, the energy employed during HCD fragmentation can be also directly scaled in eV.[24,40] Recapitulative data for the investigated species corresponding to CD-metal complexes are provided in Figure S4 and Table S2. As NCE takes into account the mass difference between the complexes (i.e., the higher mass, the larger energy is applied), observed variations in CE_{50} should reflect influence of structural features of the various CDs-transition metal binary complexes. For α-CD, SY curves and deduced CE_{50} in eV values allow to establish the following stability ranking towards metals: $Ni^{2+} > Mn^{2+}$, $Cu^{2+} > Co^{2+} > Zn^{2+} > Fe^{2+}$ (Table S2). A different behavior was observed for β-CD, for which the following trend was determined: $Mn^{2+} > Ni^{2+} > Co^{2+} \approx Zn^{2+} > Fe^{2+} >> Cu^{2+}$, and also for γ-CD-metals complexes, for which the stability preference was: $Mn^{2+} > Ni^{2+} > Co^{2+} > Fe^{2+} > Zn^{2+} >> Cu^{2+}$. Such observation associating the decreasing of the metal affinity with increasing rigidity of the host molecule, was reported elsewhere by calculations.[36]

To gain more insights into the stability of the complexes toward dissociation, we have chosen to focus on the energetics of one fragmentation process occurring for all ions and corresponding to the loss of one glucose unit via a double C-O-C glycosidic bond cleavage. Such fragmentation was previously reported in the literature for linear and branched oligosaccharides.[51] As the CD rim is constituted by several glucose units which are nonequivalent as they are more or less close to the metal ion, bond dissociation energies (BDEs) were determined for the loss of each unit in the rim as the electronic energy variation between the (n-1) rim + the glucose unit and the (n)-rim (Scheme 1 and Table S3).

Nonetheless, the values differences in BDEs span over a large range (several tenths of kcal/mol) which suggests a more and less strong interaction between the glucose and the metal. For all metals, the furthest the position to the metal cation, the lowest BDEs, the easiest the glucose unit is removed. Otherwise for a given CD, the lowest BDEs with every metals span over 6.0, 9.3 and 7.5 $kcal.mol^{-1}$ between the weakest and the strongest bond for α-CD, β-CD and γ-CD, respectively (Table 3 and S3). Such relatively well-sized variation depicts very well the subtle difference according to each CD-metal couples. However, detailed analysis of BDEs allows establishing the following ranking for α-CD: $Cu^{2+} \approx Co^{2+} > Zn^{2+} > Fe^{2+} > Mn^{2+} > Ni^{2+}$; β-CD: Fe^{2+}

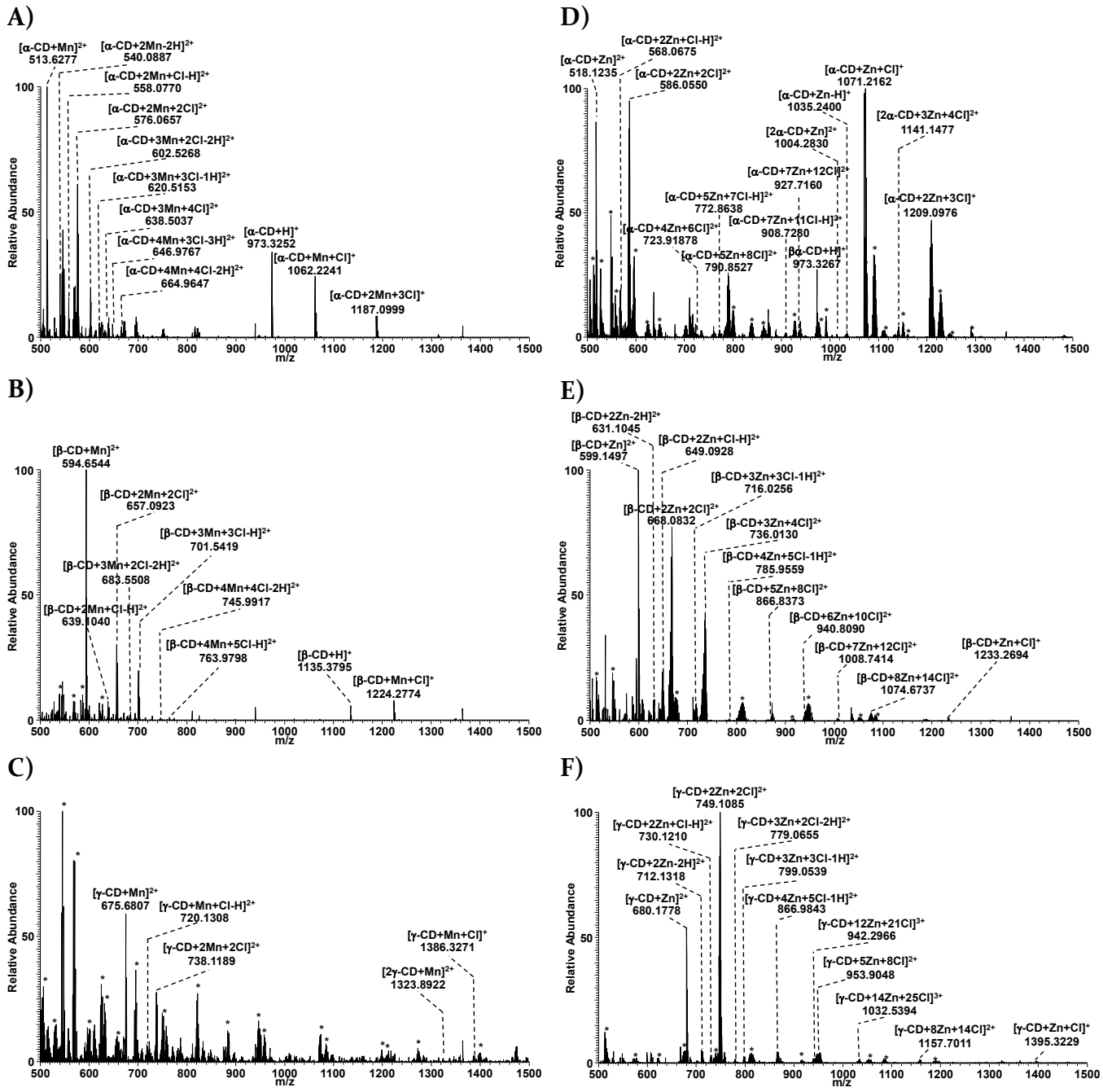

Figure 2. Mass spectra of (A) α-, (B) β- and (C) γ-CD associated with $MnCl_2$, or with $ZnCl_2$ ((D), (E) and (F), respectively). Cyclodextrin and metal chloride were at 10 µ.mol.L^{-1} and 100 µ.mol.L^{-1}, respectively. Asterisks represent metal chloride clusters.

> Mn^{2+} > Ni^{2+} > Co^{2+} > Cu^{2+} ≈ Zn^{2+} and γ-CD: Ni^{2+} > Co^{2+} > Cu^{2+} ≈ Fe^{2+} > Zn^{2+} > Mn^{2+}.

To tentatively explain the differences between ranking from BDEs and CE_{50} values, MS/MS spectra resulting from CE_{50} were further examined. A particular attention was paid to the identification of each fragment appearing at an energy below CE_{50} values. Spectra highlight that metal complexes upon HCD dissociation did not yield exclusive and/or most abundant fragment corresponding to loss of glucose unit. This suggests that BDEs values only cannot serve as relevant feature to serve as the only molecular descriptor for all studied transition metals-based edifices. Indeed, fragments corresponding to precursor with loss of 1 or 2 water molecules, as well as single charge reduction (electron capture due to excitation/dissociation processes), were frequently observed. Consequently, the corresponding BDEs should thus also be included to getthe most relevant description of the fragmentation processes. Interestingly, such mechanisms are particularly present with $[CD+Cu]^{2+}$ complexes. The distinctive behavior of Cu^{2+} could be connected with its $3d^9 4s^2$ electron

Table 2. Binding energies (E_{ass}) of the most stable CD + metal complex obtained at the y B3LYP/ Def2-SV(P) level of theory.

Metal	α-CD				β-CD				γ-CD			
	NCP[a]	BL (Å)[b]	E_{ass} (kcal.mol^{-1})	Conformer[c]	NCP[a]	BL (Å)[b]	E_{ass} (kcal.mol^{-1})	Conformer[c]	NCP[a]	BL (Å)[b]	E_{ass} (kcal.mol^{-1})[c]	Conformer[c]
Mn^{2+}	4	2.030	-329.4	cccw	3	1.966	-328.3	cwcw	4	2.016	-336.5	cccc
Fe^{2+}	5	2.050	-342.8	cwcw	4	1.993	-348.3	cccw	3	1.888	-356.6	cccw
Co^{2+}	4	2.060	-329.3	cwcw	3	1.944	-333.1	cwcw	3	1.958	-344.5	cwcw
Ni^{2+}	4	1.929	-377.0	cccw	3	1.861	-397.9	cwcw	3	1.856	-412.9	cwcc
Cu^{2+}	3	2.005	-355.2	cwcw	3	2.047	-358.4	cccw	3	2.042	-374.8	cwcw
Zn^{2+}	5	2.129	-326.6	cwcw	3	1.929	-340.6	cwcw	3	1.933	-344.6	cwcw

[a] NCP: Number of coordination points; [b] BL: average bond length over the three or four proximal oxygens according to NCP. [c]dd

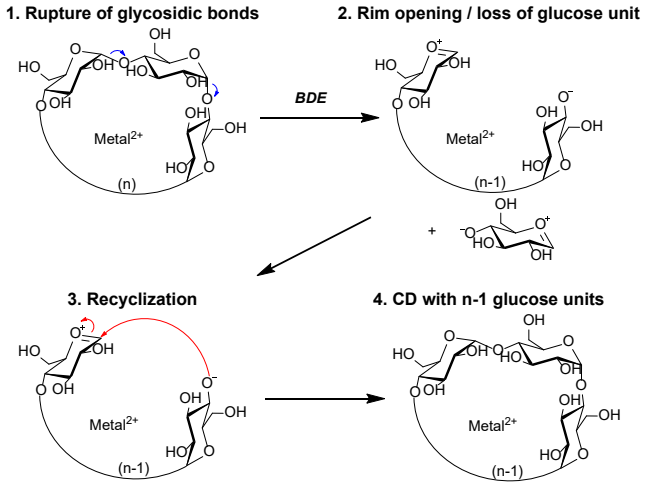

Scheme 1. Proposed mechanism for the fragmentation pathway with loss of one glucose unit in CD/metal^{2+} complexes.

configuration. In order to fill the d-shell, one electron is needed. Consequently, one may assume a one-electron transfer to occur from oxygen of CD to the Cu^{2+} cation yielding a Cu^{+} ion and a cation-radical type complex $[CD+Cu]^{+}$. Such one-electron transfer processes in the gas phase involving Cu^{2+} and yielding to cation-radical-type species were already reported in previous studies.[52–59] In addition, open-shell d-electron configurations on the metal ions, e.g. doublet states Cu^{2+}, can favor square planar structures due to Jahn-Teller stabilization with various ligands. By setting an offset considering only the fragments ascribed to one glucose loss produced during MS/MS experiment, the reprocessing of data led to corrected survival yield curves (Figure S7). Corrected data (Table 4 and figure 6) showed that the energy required to dissociate the half of precursor ion was varied in narrow range i.e. 5-7 eV.

In details, a constant increase of CE_{50} was noted from α- to β-CD and then to γ-CD with almost all metals. Some exception occurred. For instance, the Co^{2+} and Cu^{2+} complexes exhibit lower values on going from α-CD to β-CD, i.e. 21 to 19 eV and 21 to 18 eV, respectively, and the Zn^{2+} complexes afforded the same value (16 eV) for α-CD and β-CD. At a glance, the primary rim of α-CD offers a better template than β-CD and γ-CD for cobalt and copper stabilization. On the other hand, the higher flexibility of γ-CD leads to a better so-called induced-fit binding effect than β-CD. Finally, the corrected affinity order is $Co^{2+} \approx Cu^{2+} > Mn^{2+} \approx Fe^{2+} > Co^{2+} > Ni^{2+} > Zn^{2+}$, $Fe^{2+} > Mn^{2+} \approx Ni^{2+} > Co^{2+} > Cu^{2+} > Zn^{2+}$, $Ni^{2+} > Co^{2+} > Fe^{2+} \approx Cu^{2+} > Mn^{2+} > Zn^{2+}$, for α-, β- and γ-CD, respectively. Then, updated CE_{50} values match very well with the expected BDEs ranking for transition metals. It means that BDEs can serve as a suitable parameter to delineate mechanism occurring in CD-metal complexes. These results particularly highlight that: i) whatever the size of CD, Mn^{2+} and Ni^{2+} present the best affinity by far and ii) Cu^{2+} shows a strong interaction, similar to Mn^{2+} for α-CD, but slighter, compared to other studied metals, for β- and γ-CD. Although native CDs with Cu(II) are among the most studied CD/metal complexes due to their higher stability in solution, they required very particular solvent and pH conditions (see introduction). Here, analysis under gas phase (absence of solvent, different electronic effects,...) can explain such stability differences as compared to those obtained in basic solution. It was previously demonstrated that a rough correlation exists between the metal cation radius and formation enthalpy values establishing that the smaller the cationic radius is (i.e. the higher the respective charge density of the cation is), the more thermodynamically favorable the complex formation is.[36] Nevertheless, such result must be taken with many precautions since comparisons were achieved with metal series either through a given column (5 from group IIA or 2 from group IIB) or for two couples between those

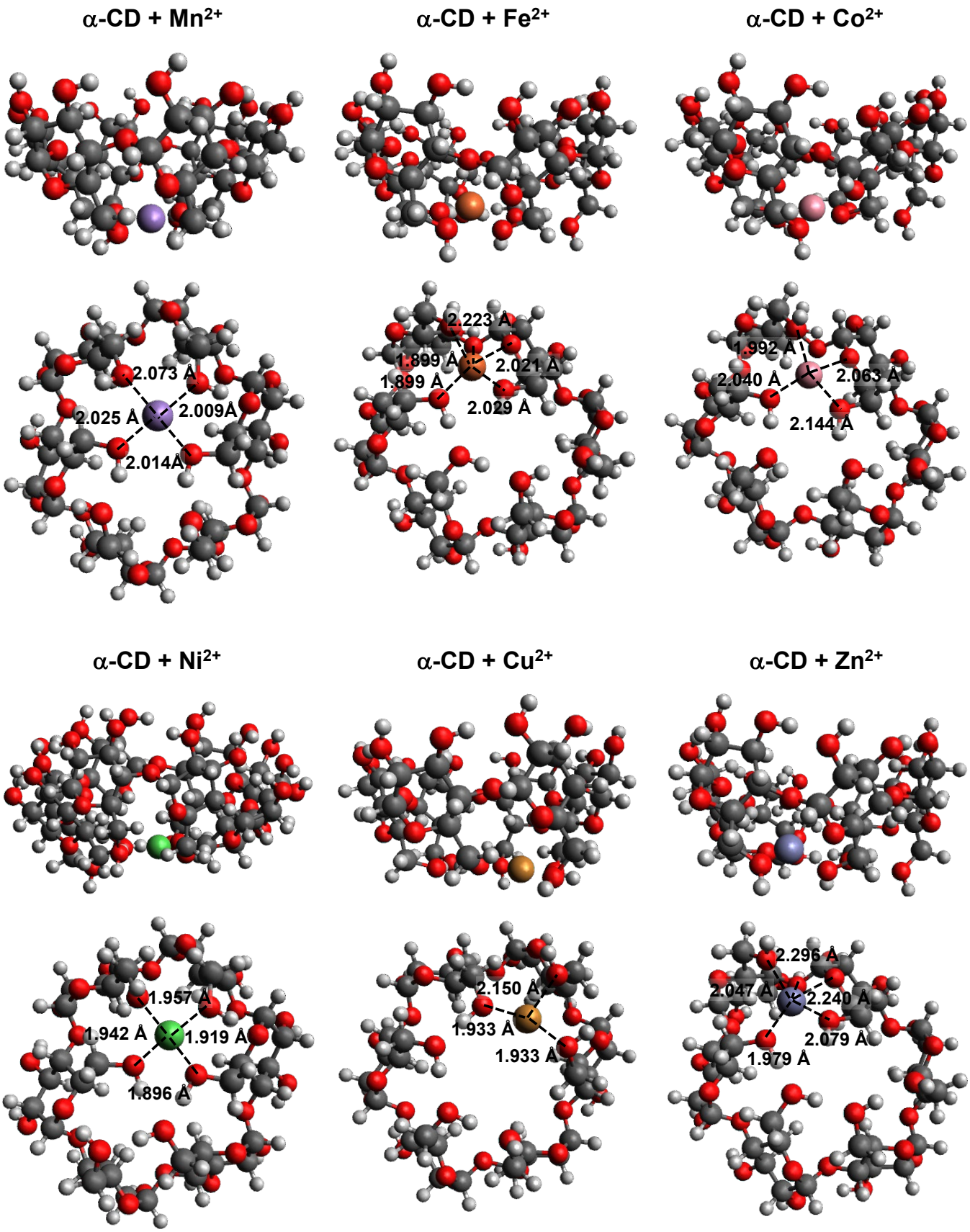

Figure 3. B3LYP/ Def2-SV(P) fully optimized structures of optimized α-CD/divalent metal 1 : 1 complexes in the gas phase (side and top views).

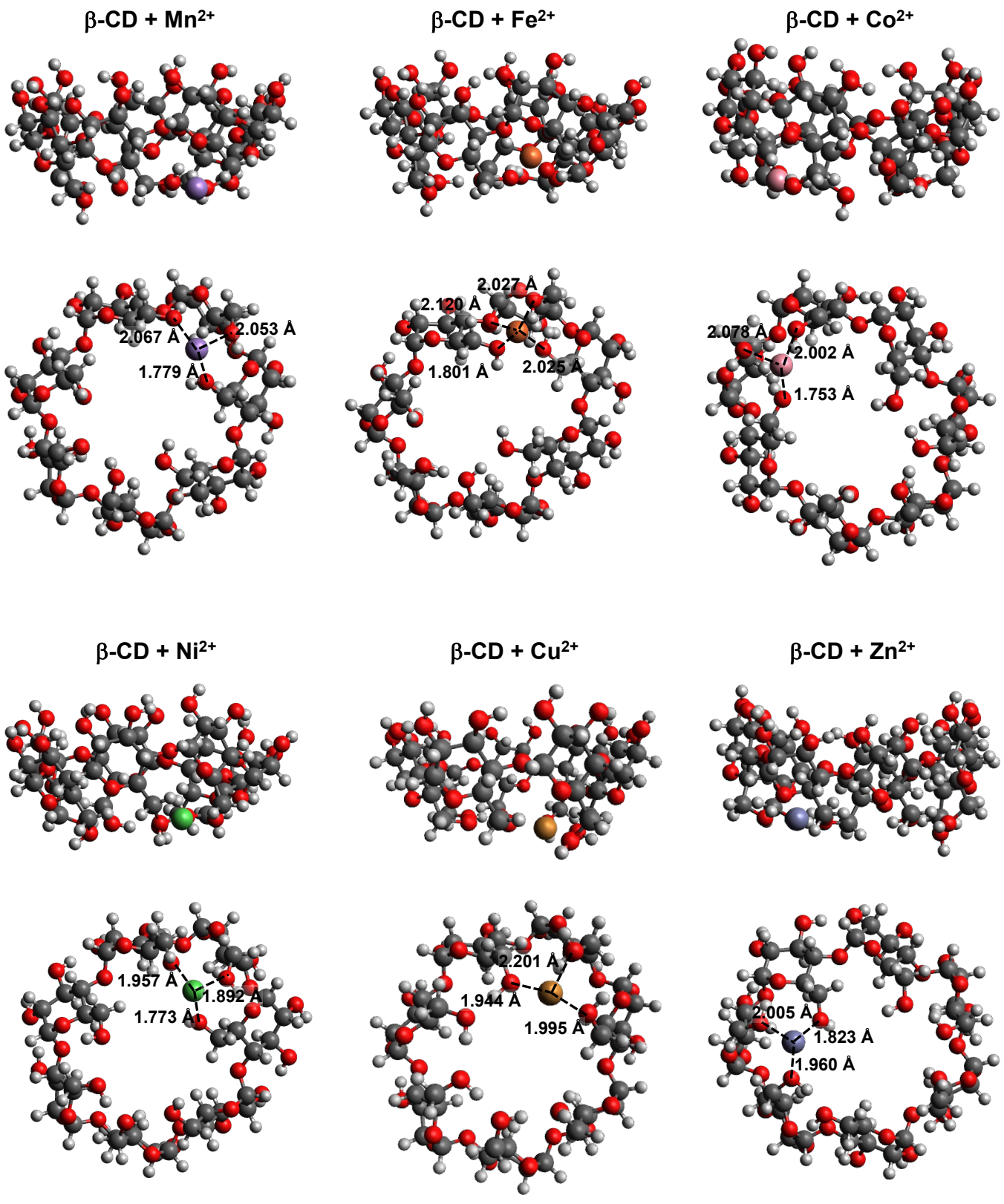

Figure 4. B3LYP/ Def2-SV(P) fully optimized structures of optimized β-CD/divalent metal 1 : 1 complexes in the gas phase (side and top views).

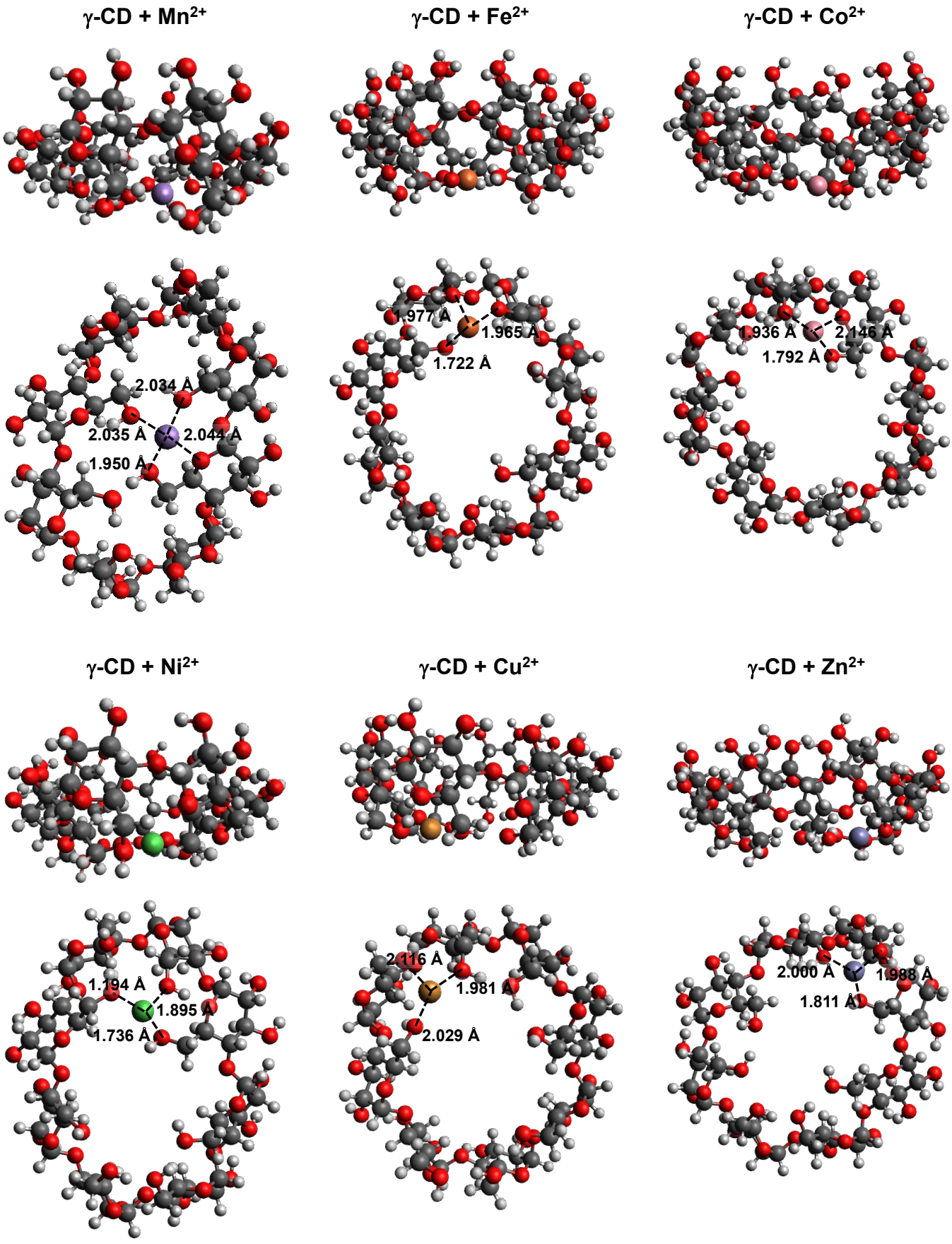

Figure 5. B3LYP/ Def2-SV(P) fully optimized structures of optimized γ-CD/divalent metal 1 : 1 complexes in the gas phase (side and top views).

Table 3. Bond dissociation energies (BDEs) obtained for the energetically most favorable glucose unit loss of the [Metal + CD]$^{2+}$ complexes (kcal.mol^{-1}) at O K.

Metal (M)	[M + α-CD]$^{2+}$	[M + β-CD]$^{2+}$	[M + γ-CD]$^{2+}$
Mn^{2+}	45.0	47.4	36.4
Fe^{2+}	46.0	49.9	40.5
Co^{2+}	50.2	41.6	42.5
Ni^{2+}	44.3	43.7	43.9
Cu^{2+}	50.3	40.9	40.2
Zn^{2+}	47.9	40.6	38.1

two groups. In our study, allmetals belong to the (post-) transition metal first raw and are consecutively distributed in group VIIB, VIIIB and IIB from manganese to zinc. Even with difference in ionic radii both under crystal (CIR: 0.61-0.83 pm, Table 1) or hydrated form (HIR: 4.04-4.38 pm, Table 1), no direct correlation can be established for the various metal-loaded CD complexes with results from binding energy, CE_{50} or BDEs values whole ranking. A similar conclusion can be drawn if taking into account the respective charge density of the cation with crystal (Z/CIR: 2.41-3.17, Table 1), or hydrated form (Z/HIR: 0.46-0.50, Table 1). As all investigated guests, metals are subjected to hybridization between their valence s-orbital and their highest occupied d-orbitals constituting very good electron density acceptors. On the other hand, numerous oxygens (hydroxyl, hemiacetal of glycosidic bond) exhibiting lone pair electrons, are present within CD, providing an important electron stock to share. Even if it is well known that the electrostatic interactions between metal and ligating oxygen atoms mainly govern the formation of carbohydrate-metal supramolecular assemblies, the question of charge spreading through the complex still remains to be addressed.

To gain further insight into topology of CD-metal complexes, a Natural Bond Orbital (NBO) analysis was performed. NBO gives access to electronic density distribution on atoms and bonds distributed among partial charge (δ) and charge transfer (CT), and herein, allows for instance to see the donor or acceptor effect of various transition metals and CDs (Table 5). For α-CD, the CT feature allows to obtain the following order: Cu^{2+} (1.105 e) > Ni^{2+} (0.989 e) > Fe^{2+} (0.939 e) > Mn^{2+}(0.748 e) > Co^{2+} (0.701 e) > Zn^{2+} (0.627 e), which completely fits with order obtained by binding energy calculation (E_{ass}) and a part of those from BDE and corrected CE_{50}. Conversely, with β- and γ-CD, the obtained orders i.e. Cu^{2+}> Fe^{2+} > Ni^{2+}> Mn^{2+} > Co^{2+} > Zn^{2+} and Cu^{2+} > Ni^{2+}> Fe^{2+} > Co^{2+} > Mn^{2+} > Zn^{2+}, respectively, fit only in part with other studied features. Data show that a direct correlation can be drawn between δ and CT of the metal and its affinity towards α-CD. Nevertheless, taking into account β- and γ-CD, results also suggest that α-CD is a particular case. Anyway, it clearly appears that the charge accepting properties of the metal cation seems to be a major determinant of the metal selectivity in CD-metal complexes. In fact, more than only a local charge transfer, the coordination of metals occurring to the narrow rim of the CD, most of

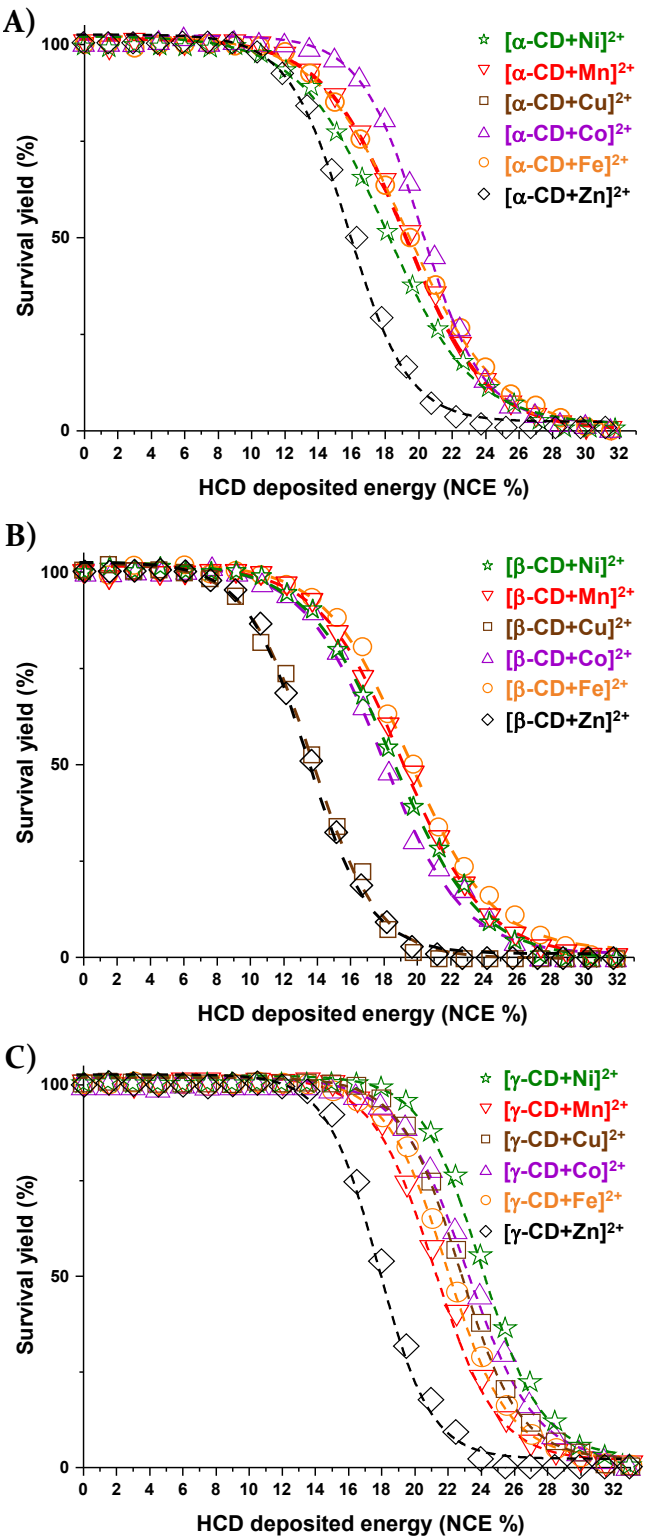

Figure 6. Survival yield curves with offset taking into account only loss of 1 glucose unit obtained for doubly charged species of α-CD (A), β-CD (B), and γ-CD (C) with the various metals upon HCD dissociation mode.

time at the edge of this last one (Figure 3-5) and with some slight variation following the Z axis (more or less deeply into the cavity), leads to obtain a particular topography for each complex. Such topography can be easily revealed by

Table 4. Recapitulative of characteristic CE_{50} values obtained for the CD- metals complexes. Standard deviation obtained for 3 m/z determinations was 0.1%.

	Metal	m/z ([CD+Metal]$^{2+}$)		Mass accuracy (ppm)	HCD CE_{50}	
		Exp.	Theo.		%	eV
α-CD	Mn^{2+}	513.6277	513.6269	1.6	19.5	20
	Fe^{2+}	514.1257	514.1254	0.6	19.6	20
	Co^{2+}	515.6249	515.6245	0.8	20.5	21
	Ni^{2+}	515.1263	515.1256	1.4	18.2	18
	Cu^{2+}	517.6237	517.6227	1.9	20.5	21
	Zn^{2+}	518.1235	518.1225	1.9	16.4	16
β-CD	Mn^{2+}	594.6544	594.6534	1.7	19.1	22
	Fe^{2+}	595.1534	595.1518	2.7	19.5	23
	Co^{2+}	596.6504	596.6509	0.8	17.9	19
	Ni^{2+}	596.1518	596.1520	0.3	18.5	22
	Cu^{2+}	598.6506	598.6491	2.5	13.8	18
	Zn^{2+}	599.1497	599.1489	1.3	13.6	16
γ-CD	Mn^{2+}	675.6807	675.6798	1.3	21.6	29
	Fe^{2+}	676.1799	676.1782	2.5	22.7	31
	Co^{2+}	677.6779	677.6773	0.9	23.6	32
	Ni^{2+}	677.1798	677.1784	2.1	24.5	33
	Cu^{2+}	679.6769	679.6755	2.1	22.4	31
	Zn^{2+}	680.1768	680.1753	2.2	18.3	24

building an electron density map of the host-guest interaction. For example, the six β-CD-metal complexes can be displayed with positively (red area, Figure 7) and negatively (blue area, Figure 7) charged sites, mainly due to the highest positive electron density of the divalent metal as guest and the highest negative electron density of the host molecule located in the vicinity of the narrow and broad rim, respectively. Then, such 3D fingerprint can be used as a tool to attempt rationalization of molecular recognition effectiveness during many processes such as drugs encapsulation/stabilization, sensor, mimetic enzyme or chemical catalysis systems, etc. Combination of i) the electronic density, ii) the three-dimensional coordinates of CDs i.e. X/Y and Z for the various oxygen involved on the primary rim and along the cone axis more and less deep in cavity, respectively, and iii) possible distortion of the structure, constitute unique topologies for each CD-metal investigated.

CONCLUSIONS

To the best of our knowledge, we report herein the most complete investigation disclosing some factors affecting the selective binding of transition metals to native α-, β- and γ-CD. Our strategy allying ESI-MS(/MS) and DFT implemented with B3LYP/Def2-SV(P) to probe both solution and gas phase selectivity and to modelize the most stable non-covalent assembly, has highlighted key features of the CD/metal coordination complex interactions. From the data obtained, it can be established a former compendium of factors governing CD-metal including, on the one hand

Table 5. NBO metal partial charge (δ) and corresponding charge transfer (CT) from CD to the metal cation in [M + CD]$^{2+}$ complexes .

CDs	Metals	δ (e)	CT (e)
α-CD	Mn^{2+}	1.252	0.748
	Fe^{2+}	1.061	0.939
	Co^{2+}	1.299	0.701
	Ni^{2+}	1.011	0.989
	Cu^{2+}	0.895	1.105
	Zn^{2+}	1.373	0.627
β-CD	Mn^{2+}	1.156	0.844
	Fe^{2+}	0.854	1.146
	Co^{2+}	1.167	0.833
	Ni^{2+}	0.947	1.053
	Cu^{2+}	0.846	1.154
	Zn^{2+}	1.320	0.680
γ-CD	Mn^{2+}	1.226	0.774
	Fe^{2+}	0.992	1.008
	Co^{2+}	1.202	0.798
	Ni^{2+}	0.976	1.024
	Cu^{2+}	0.866	1.134
	Zn^{2+}	1.311	0.689

the metal cation properties i.e. ion radius, electron configuration,coordination number or spin sate and, on the other hand, the CD flexibility and the orientation of hydroxyl groups. All these characteristics support the reorganization of this host molecule to tightly accommodate the guest metal forming an optimal 3-D binding site, illustrating very well the so-called induced-fit binding effect and insuring complex stability.[26,35] Complex formation always involved the primary OH groups sometimes assisted by hemi-acetal or glycosidic oxygens. Consecutively to the coordination of the metal, the hydrogen-bond network is disrupted, the electron density in the metal complex is redistributed and charge transfer redirected from the narrow rim towards the metal cation. This sharing is quantitate by the NBO analysis. Experimental approach with mass spectrometry reveals that the increasing flexibility of macrocycles from α- to γ-CD, as well as decreasing O-metal bond length, enhanced the binding affinity for all transition metals, which is in good agreement with binding energy calculations. Nonetheless, that is in sharp contrast with calculated BDE for glucose unit loss, revealing that other mechanisms took place such as losses of water as well as single chargereduction occurring after activation of the complexes. It has also to be kept in mind that some additional parameters, not studied here, shall also be considered such as i) the solvent effect, especially concerning its polarity since it was observedthat dielectric constant can affect the stability of complexes between carbohydrate based macrocycles with transition metals;[27,45] ii) the solvation effect, particularly with explicit water coordination in the metal;[27] iii) the effect of the amount of metal and their respective kinetics of binding/releasing, since it was described that a fine control of metal concentrations is sometimes necessary to fulfill the metal specificity in a mixture;[60] iv) the nature and presence of counterions, well known to be very important to keep or not the metallic center in solution. v) other parameters regarding the metal such as the oxophilicity and the

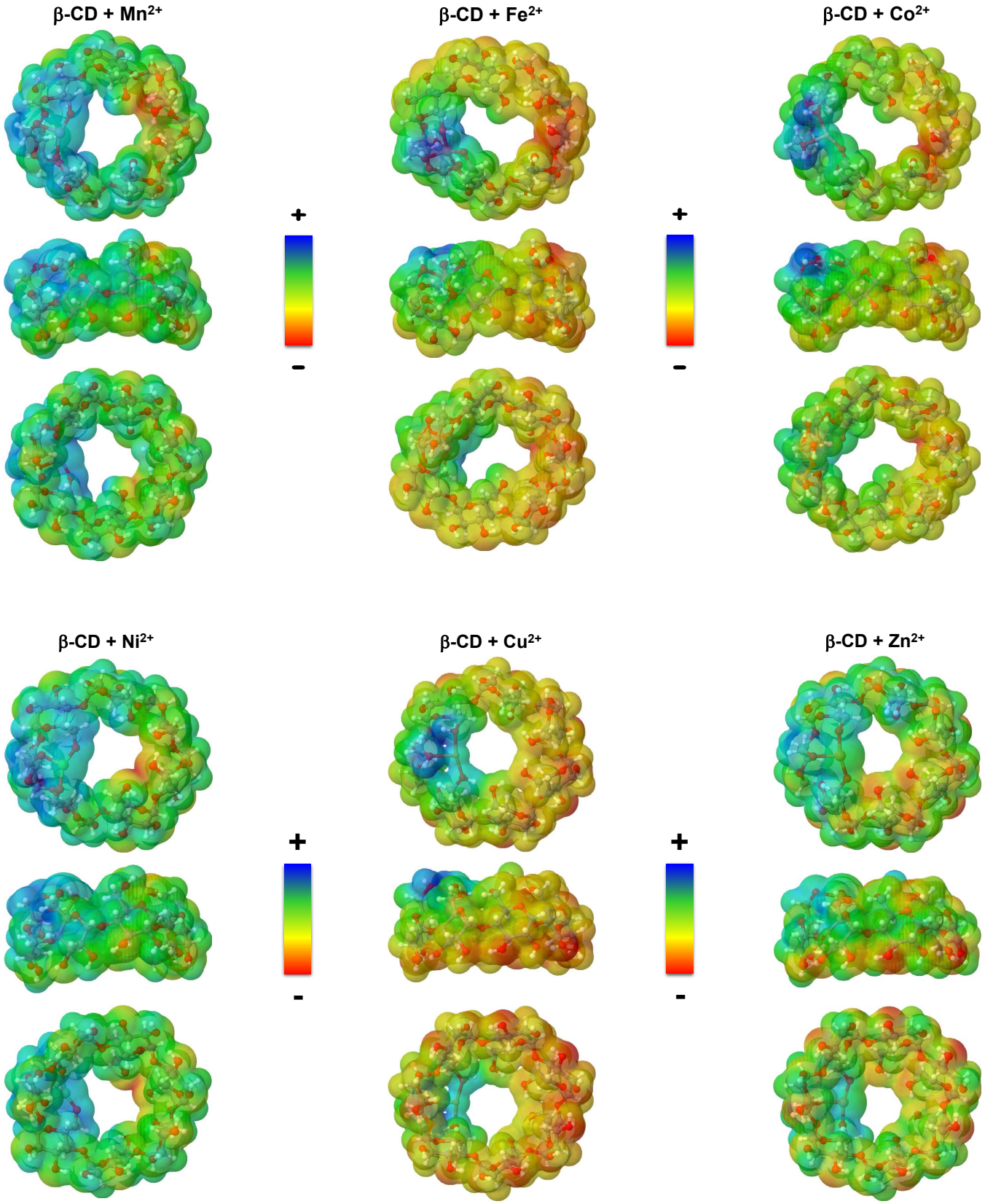

Figure 7. Top, side and bottom views of electron density of complexes between β-CD and the six studied metals (isovalue = 0.002), mapped with electrostatic potential (color scheme: red for negative surface map values and blue for the positive ones).

thiophilicity[61] or the acid softness index using Gibbs free energy of formations.[62] Hence, Cu^{2+} is reported as a soft acid and on the other hand the hardness of acid increases as follows: Ni^{2} < Co^{2+}< Fe^{2+}< Zn^{2+} < Mn^{2+}. The present work paves the way for a better rationalization of the binding mechanisms of transition metals and their selectivity in α-, β-and γ-CD although a complete understanding of these processes is not fully reached yet. The overlaying electron density and geometrical arrangement of the complexes (Figure 7) can constitute a useful first mussel to probe ternary complexes involving, for example the interaction (inclusion) of substrate during catalysis processes. Such strategy could then be further correlated with combination of docking and catalysis experiments.

ASSOCIATED CONTENT

Supporting Information

Protocol of UV-visible experiences of α-, β-and γ-CD with the studied metals and UV-visible spectra of β-CD with $Fe(Cl)_2$. Recapitulative table of the binding energy of three most stable conformers obtained between the α-, β-and γ-CD and one transition metal cation and various.by B3LYP/Def2-SV(P). ESI-Full-MS spectra of α-, β-and γ-CD with $Co(Cl)_2$, $Ni(Cl)_2$, $Fe(Cl)_2$ and Cu(Cl).(PDF) The Supporting Information is available free of charge on the ACS Publications website.

AUTHOR INFORMATION

Corresponding Author

Cédric Przybylski - *Sorbonne Université, CNRS, Institut Parisien de Chimie Moléculaire, IPCM, 4 place Jussieu, F-75005 Paris, France.* https://orcid.org/0000-0003-0352-1461; Email: cedric.przybylski@sorbonne-universite.fr

Author

Héloïse Dossmann - *Sorbonne Université, CNRS, Institut Parisien de Chimie Moléculaire, IPCM, 4 place Jussieu, F-75005 Paris, France.* https://orcid.org/0000-0003-4844-229X

Véronique Bonnet – *Université de Picardie Jules Verne, Laboratoire de Glycochimie, des Antimicrobiens et des Agroressources, LG2A, CNRS UMR 7378, 80039 Amiens, France.* https://orcid.org/0000-0002-4220-9617

Eric Monflier – *Université d'Artois, CNRS, Centrale Lille, ENSCL, Université de Lille, UMR 8181, -UCCS- Unité de Catalyse et Chimie du Solide, F-62300 Lens, France.* https://orcid.org/0000-0001-5865-0979

Anne Ponchel – *Université d'Artois, CNRS, Centrale Lille, ENSCL, Université de Lille, UMR 8181, -UCCS- Unité de Catalyse et Chimie du Solide, F-62300 Lens, France.* https://orcid.org/0000-0003-0476-7973

ACKNOWLEDGMENT

This work was granted access to the HPC resources of the HPCaVe centre at UPMC-Sorbonne Université and of IDRIS under the allocation 2019-A0050810312 made by GENCI. Both facilities are gratefully acknowledged.

REFERENCES

(1) Diéguez, M.; Pàmies, O.; Ruiz, A.; Díaz, Y.; Castillón, S.; Claver, C. Carbohydrate Derivative Ligands in Asymmetric Catalysis. *Coord. Chem. Rev.* **2004**, *248* (21), 2165–2192. https://doi.org/10.1016/j.ccr.2004.04.009.

(2) McKay, M. J.; Nguyen, H. M. Recent Advances in Transition Metal-Catalyzed Glycosylation. *ACS Catal.* **2012**, *2* (8), 1563–1595. https://doi.org/10.1021/cs3002513.

(3) Yucheng, J.; Shiyang, G.; Shuping, X.; Mancheng, H.; Jianji, W.; Yan, L.; Kelei, Z. The Enthalpy and Entropy Interaction Parameters of Cesium Chloride with Saccharides (d-Glucose, d-Fructose and Sucrose) in Water at 298.15 K. *Thermochim. Acta* **2003**, *400* (1), 37–42. https://doi.org/10.1016/S0040-6031(02)00476-8.

(4) Saladini, M.; Menabue, L.; Ferrari, E. Sugar Complexes with Metal2+ Ions: Thermodynamic Parameters of Associations of Ca2+, Mg2+ and Zn2+ with Galactaric Acid. *Carbohydr. Res.* **2001**, *336* (1), 55–61. https://doi.org/10.1016/S0008-6215(01)00243-9.

(5) Angyal, S. J. Complexes of Metal Cations with Carbohydrates in Solution. In *Advances in Carbohydrate Chemistry and Biochemistry*; Tipson, R. S., Horton, D., Eds.; Academic Press, 1989; Vol. 47, pp 1–43. https://doi.org/10.1016/S0065-2318(08)60411-4.

(6) Dodziuk, H. *Cyclodextrins and Their Complexes: Chemistry, Analytical Methods, Applications*, Wiley VCH.; Weinheim.

(7) Szejtli, J. Introduction and General Overview of Cyclodextrin Chemistry. *Chem. Rev.* **1998**, *98* (5), 1743–1754. https://doi.org/10.1021/cr970022c.

(8) Crini, G. Review: A History of Cyclodextrins. *Chem. Rev.* **2014**, *114* (21), 10940–10975. https://doi.org/10.1021/cr500081p.

(9) Connors, K. A. The Stability of Cyclodextrin Complexes in Solution. *Chem. Rev.* **1997**, *97* (5), 1325–1358. https://doi.org/10.1021/cr960371r.

(10) Rekharsky, M. V.; Inoue, Y. Complexation Thermodynamics of Cyclodextrins. *Chem. Rev.* **1998**, *98* (5), 1875–1918. https://doi.org/10.1021/cr9700150.

(11) Norkus, E. Metal Ion Complexes with Native Cyclodextrins. An Overview. *J. Incl. Phenom. Macrocycl. Chem.* **2009**, *65* (3), 237. https://doi.org/10.1007/s10847-009-9586-x.

(12) Tomer, A.; Wyrwalski, F.; Przybylski, C.; Paul, J.-F.; Monflier, E.; Pera-Titus, M.; Ponchel, A. Facile Preparation of Ni/Al2O3 Catalytic Formulations with the Aid of Cyclodextrin Complexes: Towards Highly Active and Robust Catalysts for the Direct Amination of Alcohols. *J. Catal.* **2017**, *356*, 111–124. https://doi.org/10.1016/j.jcat.2017.10.006.

(13) Noël, S.; Léger, B.; Ponchel, A.; Philippot, K.; Denicourt-Nowicki, A.; Roucoux, A.; Monflier, E. Cyclodextrin-Based Systems for the Stabilization of Metallic(0) Nanoparticles and Their Versatile Applications in Catalysis. *Recent Dev. Catal. Des. Act.* **2014**, *235*, 20–32. https://doi.org/10.1016/j.cattod.2014.03.030.

(14) Polarz, S.; Smarsly, B.; Bronstein, L.; Antonietti, M. From Cyclodextrin Assemblies to Porous Materials by Silica Templating. *Angew. Chem. Int. Ed.* **2001**, *40* (23), 4417–4421. https://doi.org/10.1002/1521-3773(20011203)40:23<4417::AID-ANIE4417>3.0.CO;2-P.

(15) Prochowicz, D.; Kornowicz, A.; Lewiński, J. Interactions of Native Cyclodextrins with Metal Ions and Inorganic Nanoparticles: Fertile Landscape for Chemistry and Materials Science. *Chem. Rev.* **2017**, *117* (22), 13461–13501. https://doi.org/10.1021/acs.chemrev.7b00231.

(16) Bellia, F.; La Mendola, D.; Pedone, C.; Rizzarelli, E.; Saviano, M.; Vecchio, G. Selectively Functionalized Cyclodextrins and Their Metal Complexes. *Chem Soc Rev* **2009**, *38* (9), 2756–2781. https://doi.org/10.1039/B718436K.

(17) Rebilly, J.-N.; Colasson, B.; Bistri, O.; Over, D.; Reinaud, O. Biomimetic Cavity-Based Metal Complexes. *Chem Soc Rev* **2015**, *44* (2), 467–489. https://doi.org/10.1039/C4CS00211C.

(18) Bistri, O.; Reinaud, O. Supramolecular Control of Transition Metal Complexes in Water by a Hydrophobic Cavity: A Bio-Inspired Strategy. *Org Biomol Chem* **2015**, *13* (10), 2849–2865. https://doi.org/10.1039/C4OB02511C.

(19) Xu, G.; Leloux, S.; Zhang, P.; Meijide Suárez, J.; Zhang, Y.; Derat, E.; Ménand, M.; Bistri-Aslanoff, O.; Roland, S.; Leyssens, T.; Riant, O.; Sollogoub, M. Capturing the Monomeric (L)CuH in NHC-Capped Cyclodextrin: Cavity-Controlled Chemoselective Hydrosilylation of α,β-Unsaturated Ketones. *Angew. Chem. Int. Ed.* **2020**, *59* (19), 7591–7597. https://doi.org/10.1002/anie.202001733.

(20) Bartsch, H.; König, W. A.; Straβner, M.; Hintze, U. Quantitative Determination of Native and Methylated Cyclodextrins by Matrix-Assisted Laser Desorption/Ionization Time-of-Flight Mass Spectrometry. *Carbohydr. Res.* **1996**, *286*, 41–53. https://doi.org/10.1016/0008-6215(96)00049-3.

(21) Bashir, S.; Derrick, P. J.; Critchley, P.; Gates, P. J.; Staunton, J. Matrix-Assisted Laser Desorption/Ionization Time-of-Flight Mass Spectrometry of Dextran and Dextrin Derivatives. *Eur. J. Mass Spectrom. Chichester Engl.* **2003**, *9* (1), 61–70. https://doi.org/10.1255/ejms.510.

(22) Choi, S.-S.; Lee, H. M.; Jang, S.; Shin, J. Comparison of Ionization Behaviors of Ring and Linear Carbohydrates in MALDI-TOFMS. *Int. J. Mass Spectrom.* **2009**, *279* (1), 53–58. https://doi.org/10.1016/j.ijms.2008.10.007.

(23) Reale, S.; Teixidò, E.; de Angelis, F. Study of Alkali Metal Cations Binding Selectivity of β-Cyclodextrin by ESI-MS. *Ann. Chim.* **2005**, *95* (6), 375–381. https://doi.org/10.1002/adic.200590057.

(24) Przybylski, C.; Bonnet, V.; Cézard, C. Probing the Common Alkali Metal Affinity of Native and Variously Methylated β-Cyclodextrins by Combining Electrospray-Tandem Mass Spectrometry and Molecular Modeling. *Phys Chem Chem Phys* **2015**, *17* (29), 19288–19305. https://doi.org/10.1039/C5CP02895G.

(25) Frański, R.; Gierczyk, B.; Schroeder, G.; Beck, S.; Springer, A.; Linscheid, M. Mass Spectrometric Decompositions of Cationized β-Cyclodextrin. *Carbohydr. Res.* **2005**, *340* (8), 1567–1572. https://doi.org/10.1016/j.carres.2005.03.014.

(26) Stachowicz, A.; Styrcz, A.; Korchowiec, J.; Modaressi, A.; Rogalski, M. DFT Studies of Cation Binding by β-Cyclodextrin. *Theor. Chem. Acc.* **2011**, *130* (4), 939–953. https://doi.org/10.1007/s00214-011-1014-9.

(27) Angelova, S. E.; Nikolova, V. K.; Dudev, T. M. Determinants of the Host–Guest Interactions between α-, β- and γ-Cyclodextrins and Group IA, IIA and IIIA Metal Cations: A DFT/PCM Study. *Phys Chem Chem Phys* **2017**, *19* (23), 15129–15136. https://doi.org/10.1039/C7CP01253E.

(28) Nies, D. H. The Biological Chemistry of the Transition Metal "Transportome" of Cupriavidus Metallidurans. *Metallomics* **2016**, *8* (5), 481–507. https://doi.org/10.1039/C5MT00320B.

(29) Yamakawa, T.; Nishimura, S. Liquid Formulation of a Novel Non-Fluorinated Topical Quinolone, T-3912, Utilizing the Synergic Solubilizing Effect of the Combined Use of Magnesium Ions and Hydroxypropyl-β-Cyclodextrin. *J. Controlled Release* **2003**, *86* (1), 101–113. https://doi.org/10.1016/S0168-3659(02)00367-X.

(30) He, Z.; Wang, Z.; Zhang, H.; Pan, X.; Su, W.; Liang, D.; Wu, C. Doxycycline and Hydroxypropyl-β-Cyclodextrin Complex in Poloxamer Thermal Sensitive Hydrogel for Ophthalmic Delivery. *Acta Pharm. Sin. B* **2011**, *1* (4), 254–260. https://doi.org/10.1016/j.apsb.2011.10.004.

(31) Suresh, P.; Azath, I. A.; Pitchumani, K. Naked-Eye Detection of Fe3+ and Ru3+ in Water: Colorimetric and Ratiometric Sensor Based on per-6-Amino-β-Cyclodextrin/p-Nitrophenol. *Sens. Actuators B Chem.* **2010**, *146* (1), 273–277. https://doi.org/10.1016/j.snb.2010.02.047.

(32) Hapiot, F.; Tilloy, S.; Monflier, E. Cyclodextrins as Supramolecular Hosts for Organometallic Complexes. *Chem. Rev.* **2006**, *106* (3), 767–781. https://doi.org/10.1021/cr050576c.

(33) Zhang, Y.; Xu, W. The Aldol Condensation Catalyzed by Metal(II)-β-Cyclodextrin Complexes. *Synth. Commun.* **1989**, *19* (7–8), 1291–1296. https://doi.org/10.1080/00397918908054536.

(34) Defaye, J.; Crouzy, S.; Evrard, N.; Law, H. Region-Selective Method for Preparing Cyclodextrin C-6 Monosulphonyl Derivatives. WO 99/61483, 1999.

(35) Johnson, M. D.; Bernard, J. G. Hydrogen Bonding Effects on the Cyclodextrin Encapsulation of Transition Metal Complexes: 'Molecular Snaps.' *Chem Commun* **1996**, No. 2, 185–186. https://doi.org/10.1039/CC9960000185.

(36) Angelova, S.; Nikolova, V.; Molla, N.; Dudev, T. Factors Governing the Host–Guest Interactions between IIA/IIB Group Metal Cations and α-Cyclodextrin: A DFT/CDM Study. *Inorg. Chem.* **2017**, *56* (4), 1981–1987. https://doi.org/10.1021/acs.inorgchem.6b02564.

(37) Kurokawa, G.; Sekii, M.; Ishida, T.; Nogami, T. Crystal Structure of a Molecular Complex from Native β-Cyclodextrin and Copper(II) Chloride. *Supramol. Chem.* **2004**, *16* (5), 381–384. https://doi.org/10.1080/10610270420000220742.

(38) Velasco, M. I.; Krapacher, C. R.; de Rossi, R. H.; Rossi, L. I. Structure Characterization of the Non-Crystalline Complexes of Copper Salts with Native Cyclodextrins. *Dalton Trans.* **2016**, *45* (26), 10696–10707. https://doi.org/10.1039/C6DT01468B.

(39) Nightingale, E. R. Phenomenological Theory of Ion Solvation. Effective Radii of Hydrated Ions. *J. Phys. Chem.* **1959**, *63* (9), 1381–1387. https://doi.org/10.1021/j150579a011.

(40) Przybylski, C.; Bonnet, V. Discrimination of Cyclic and Linear Oligosaccharides by Tandem Mass Spectrometry Using Collision-Induced Dissociation (CID), Pulsed-Q-Dissociation (PQD) and the Higher-Energy C-Trap Dissociation Modes. *Rapid Commun. Mass Spectrom.* **2013**, *27* (1), 75–87. https://doi.org/10.1002/rcm.6422.

(41) *Gaussian 09, Revision D.01,* Frisch, M. J.; Trucks, G. W.; Schlegel, H. B.; Scuseria, G. E.; Robb, J. R.; Cheeseman, M. A.; Scalmani, G.; Barone, V.; Mennucci, B.; Petersson, G. A.; Nakatsuji, H.; Caricato, M.; Li, X.; Hratchian, H. P.; Izmaylov, A. F.; Bloino, J.; Zheng, G.; Sonnenberg, J. L.; Hada, M.; Ehara, M.; Toyota, K.; Fukuda, R.; Hasegawa, J.; Ishida, M.; Nakajima, T.; Honda, Y.; Kitao, O.; Nakai, H.; Vreven, T.; Montgomery Jr., J. A.; Peralta, J. E.; Ogliaro, F.; Bearpark, M.; Heyd, J. J.; Brothers, E.; Kudin, K. N.; Staroverov, V. N.; Kobayashi, R.; Normand, J.; Raghavachari, K.; Rendell, A.; Burant, J. C.; Iyengar, S. S.; Tomasi, J.; Cossi, M.; Rega,N.; Millam, J. M.; Klene, M.; Knox, J. E.; Cross, J. B.; Bakken, J. B.; Adamo, C.; Jaramillo, J.; Gomperts, R.; Stratmann, R. E.; Yazyev, O.; Austin, A. J.; Cammi, R.; Pomelli, C.; Ochterski, J. W.; Martin, R. L.; Morokuma, K.; Zakrzewski, V. G.; Voth, G. A.; Salvador, P.; Dannenberg, J. J.; Dapprich, S.; Daniels, A. D.; Farkas, Ö.; Foresman, J. B.; Ortiz, J. V.; Cioslowski, J.;Fox, D. J. *Gaussian, Inc., Wallingford CT, 2009.*

(42) Snor, W.; Liedl, E.; Weiss-Greiler, P.; Karpfen, A.; Viernstein, H.; Wolschann, P. On the Structure of Anhydrous β-Cyclodextrin. *Chem. Phys. Lett.* **2007**, *441* (1), 159–162. https://doi.org/10.1016/j.cplett.2007.05.007.

(43) Weigend, F.; Ahlrichs, R. Balanced Basis Sets of Split Valence, Triple Zeta Valence and Quadruple Zeta Valence Quality for H to Rn: Design and Assessment of Accuracy. *Phys Chem Chem Phys* **2005**, *7* (18), 3297–3305. https://doi.org/10.1039/B508541A.

(44) Bai, L.; Wyrwalski, F.; Safariamin, M.; Bleta, R.; Lamonier, J.-F.; Przybylski, C.; Monflier, E.; Ponchel, A. Cyclodextrin-Cobalt (II) Molecule-Ion Pairs as Precursors to Active Co3O4/ZrO2 Catalysts for the Complete Oxidation of Formaldehyde: Influence of the Cobalt Source. *J. Catal.* **2016**, *341*, 191–204. https://doi.org/10.1016/j.jcat.2016.07.006.

(45) Wang, L.; Chai, Y.; Sun, C.; Armstrong, D. W. Complexation of Cyclofrunctans with Transition Metal Ions Studied by Electrospray Ionization Mass Spectrometry and Collision-Induced Dissociation. *Int. J. Mass Spectrom.* **2012**, *323–324*, 21–27. https://doi.org/10.1016/j.ijms.2012.06.003.

(46) Kenttämaa, H. I.; Cooks, R. G. Internal Energy Distributions Acquired through Collisional Activation at Low and High

Energies. *Int. J. Mass Spectrom. Ion Process.* **1985**, *64* (1), 79–83. https://doi.org/10.1016/0168-1176(85)85038-2.

(47) Memboeuf, A.; Nasioudis, A.; Indelicato, S.; Pollreisz, F.; Kuki, Á.; Kéki, S.; van den Brink, O. F.; Vékey, K.; Drahos, L. Size Effect on Fragmentation in Tandem Mass Spectrometry. *Anal. Chem.* **2010**, *82* (6), 2294–2302. https://doi.org/10.1021/ac902463q.

(48) Nasioudis, A.; Memboeuf, A.; Heeren, R. M. A.; Smith, D. F.; Vékey, K.; Drahos, L.; van den Brink, O. F. Discrimination of Polymers by Using Their Characteristic Collision Energy in Tandem Mass Spectrometry. *Anal. Chem.* **2010**, *82* (22), 9350–9356. https://doi.org/10.1021/ac101936v.

(49) Kertesz, T. M.; Hall, L. H.; Hill, D. W.; Grant, D. F. CE50: Quantifying Collision Induced Dissociation Energy for Small Molecule Characterization and Identification. *J. Am. Soc. Mass Spectrom.* **2009**, *20* (9), 1759–1767. https://doi.org/10.1016/j.jasms.2009.06.002.

(50) Memboeuf, A.; Jullien, L.; Lartia, R.; Brasme, B.; Gimbert, Y. Tandem Mass Spectrometric Analysis of a Mixture of Isobars Using the Survival Yield Technique. *J. Am. Soc. Mass Spectrom.* **2011**, *22* (10), 1744. https://doi.org/10.1007/s13361-011-0195-8.

(51) Kováčik, V.; Hirsch, J.; Kováč, P.; Heerma, W.; Thomas-Oates, J.; Haverkamp, J. Oligosaccharide Characterization Using Collision-Induced Dissociation Fast Atom Bombardment Mass Spectrometry: Evidence for Internal Monosaccharide Residue Loss. *J. Mass Spectrom.* **1995**, *30* (7), 949–958. https://doi.org/10.1002/jms.1190300704.

(52) Barlow, C. K.; Wee, S.; McFadyen, W. D.; O'Hair, R. A. J. Designing Copper(II) Ternary Complexes to Generate Radical Cations of Peptides in the Gas Phase: Role of the Auxiliary Ligand. *Dalton Trans.* **2004**, No. 20, 3199–3204. https://doi.org/10.1039/B409687H.

(53) Karnezis, A.; Barlow, C. K.; O'Hair, R. A. J.; McFadyen, W. D. Peptide Derivatization as a Strategy to Form Fixed-Charge Peptide Radicals. *Rapid Commun. Mass Spectrom.* **2006**, *20* (19), 2865–2870. https://doi.org/10.1002/rcm.2671.

(54) Wee, S.; O'Hair, R. A. J.; McFadyen, W. D. Comparing the Gas-Phase Fragmentation Reactions of Protonated and Radical Cations of the Tripeptides GXR. *Int. J. Mass Spectrom.* **2004**, *234* (1), 101–122. https://doi.org/10.1016/j.ijms.2004.02.018.

(55) Laskin, J.; Futrell, J. H.; Chu, I. K. Is Dissociation of Peptide Radical Cations an Ergodic Process? *J. Am. Chem. Soc.* **2007**, *129* (31), 9598–9599. https://doi.org/10.1021/ja073748r.

(56) Chu, I. K.; Rodriguez, C. F.; Hopkinson, A. C.; Siu, K. W. M.; Lau, T.-C. Formation of Molecular Radical Cations of Enkephalin Derivatives via Collision-Induced Dissociation of Electrospray-Generated Copper (II) Complex Ions of Amines and Peptides. *J. Am. Soc. Mass Spectrom.* **2001**, *12* (10), 1114–1119. https://doi.org/10.1016/S1044-0305(01)00297-5.

(57) Chu, I. K.; Siu, S. O.; Lam, C. N. W.; Chan, J. C. Y.; Rodriquez, C. F. Formation of Molecular Radical Cations of Aliphatic Tripeptides from Their Complexes with CuII(12-Crown-4). *Rapid Commun. Mass Spectrom.* **2004**, *18* (16), 1798–1802. https://doi.org/10.1002/rcm.1551.

(58) Duncombe, B. J.; Duale, K.; Buchanan-Smith, A.; Stace, A. J. The Solvation of Cu2+ with Gas-Phase Clusters of Water and Ammonia. *J. Phys. Chem. A* **2007**, *111* (24), 5158–5165. https://doi.org/10.1021/jp07172l86.

(59) Felder, T.; Röhrich, A.; Stephan, H.; Schalley, C. A. Fragmentation Reactions of Singly and Doubly Protonated Thiourea- and Sugar-Substituted Cyclams and Their Transition-Metal Complexes. *J. Mass Spectrom.* **2008**, *43* (5), 651–663. https://doi.org/10.1002/jms.1365.

(60) Osman, D.; Foster, A. W.; Chen, J.; Svedaite, K.; Steed, J. W.; Lurie-Luke, E.; Huggins, T. G.; Robinson, N. J. Fine Control of Metal Concentrations Is Necessary for Cells to Discern Zinc from Cobalt. *Nat. Commun.* **2017**, *8* (1), 1884. https://doi.org/10.1038/s41467-017-02085-z.

(61) Kepp, K. P. A Quantitative Scale of Oxophilicity and Thiophilicity. *Inorg. Chem.* **2016**, 55 (18), 9461–9470. https://doi.org/10.1021/acs.inorgchem.6b01702.

(62) Xu, H.; Xu, D. C.; Wang, Y. Natural Indices for the Chemical Hardness/Softness of Metal Cations and Ligands. *ACS Omega* **2017**, *2* (10), 7185–7193. https://doi.org/10.1021/acsomega.7b01039.

Insert Table of Contents artwork here